



Heterogeneous & Homogeneous & Bio- & Nano-

CHEM **CAT** CHEM

CATALYSIS

Accepted Article

Title: Ethanol as a Binder to Fabricate a Highly-Efficient Capsule-Structured CuO-ZnO-Al₂O₃@HZSM-5 Catalyst for Direct Production of Dimethyl Ether from Syngas

Authors: Yongle Guo and Zhongkui Zhao

This manuscript has been accepted after peer review and appears as an Accepted Article online prior to editing, proofing, and formal publication of the final Version of Record (VoR). This work is currently citable by using the Digital Object Identifier (DOI) given below. The VoR will be published online in Early View as soon as possible and may be different to this Accepted Article as a result of editing. Readers should obtain the VoR from the journal website shown below when it is published to ensure accuracy of information. The authors are responsible for the content of this Accepted Article.

To be cited as: *ChemCatChem* 10.1002/cctc.201901938

Link to VoR: <http://dx.doi.org/10.1002/cctc.201901938>

WILEY-VCH

www.chemcatchem.org



Ethanol as a Binder to Fabricate a Highly-Efficient Capsule-Structured CuO-ZnO-Al₂O₃@HZSM-5 Catalyst for Direct Production of Dimethyl Ether from Syngas

Yongle Guo and Zhongkui Zhao*

Abstract: This work reports a highly efficient capsule-structured CuO-ZnO-Al₂O₃@HZSM-5 (CZA@HZSM-5-EtOH) core-shell catalyst for the direct conversion of syngas to dimethyl ether by a facile physical coating method with ethanol as a binder through coating micrometer-sized HZSM-5 shell on the prior-shaped millimeter-sized CZA core, it shows 2.9 times higher CO conversion with the 2.7 times higher turnover frequency and 9.2 times higher dimethyl ether space-time yield of the CZA@HZSM-5-SS catalyst prepared by a similar process but with silica sol as a binder (315.5 vs 34.3 g_{DME} kg_{cat}⁻¹ h⁻¹). The relationship between the structure and performance was explored by a variety of characterization techniques including X-ray diffraction (XRD), scanning electron microscope (SEM), energy dispersive spectrometer (EDS), X-ray diffraction (XRD), ammonia temperature programmed desorption (NH₃-TPD), nitrogen adsorption-desorption, H₂-temperature-programmed reduction (H₂-TPR) and H₂-TPR after oxidation of the samples by N₂O. CZA@HZSM-5-EtOH can be considered as a highly efficient and practical catalyst for dimethyl ether synthesis from syngas. This work presents a new avenue to design other bifunctional catalysts for the cascade reactions in which the raw materials can be converted into an intermediate over the core and then the as-formed intermediate over the core can be subsequently converted into the final product.

It has become a consensus to seek clean energy to replace fossil fuel because the latter is liable to pollute the environment.^[1] Dimethyl ether (DME) is expected to replace liquefied petroleum gas (LPG) for its alike physicochemical nature. In addition, DME can also be employed as an eco-friendly replacement for diesel because of its high cetane number and low emission of toxic compounds in the outlet gas. In addition, DME is an important chemical intermediate to synthesize useful chemicals (methyl acetate, methyl carbamate and dimethylsulfate).^[2-4]

Currently, the industrial synthesis of DME is carried out in a two-step process. Syngas-to-methanol reaction is performed over copper-based catalysts (mainly, Cu-ZnO-Al₂O₃) in the first step, which is thermodynamic equilibrium limitation at high reaction temperature.^[4-6] Methanol-to-DME reaction is carried out over solid acid catalysts such as acidic zeolites (HZSM-5,

HZSM-22, HY, and H-SAPO),^[7-12] γ -alumina,^[13-15] heteropolyacid,^[16,17] and mixed metal oxides^[18-20] in the second step. However, methanol, as a relatively high-cost chemical, increases the cost for producing DME, besides the two-step DME synthesis is limited by the availability of methanol.^[2] On the contrary, syngas is cheap raw material and can be available from coal gasification, biomass gasification and natural gas partial oxidation or reforming. The direct syngas-to-DME (STD) via a single process has an economic strength. Moreover, the STD process is more thermodynamically favorable, because the thermodynamic equilibrium limitation of syngas-to-methanol process can be broken by the subsequent the methanol dehydration process. Therefore, the STD route has drawn great attention of worldwide researchers from 1990's.^[2-4,21-30]

The hybrid catalysts prepared by physically mixing methanol synthesis catalyst (Cu-ZnO-Al₂O₃) and methanol dehydration catalyst (solid acid) were attempted to catalyze the STD process.^[31-40] The methanol synthesis unit in the hybrid catalysts have been focused on tuning catalysts composition,^[21-25] synthetic method,^[26,27] preparation parameters of Cu-based catalysts^[28,29] and alternatives to Cu-based.^[30] The methanol dehydration unit in the hybrid catalysts has been focused on the modulation of particle size^[31], structure^[32-34] and modification of acidic sites by metal^[35-38] of zeolite and γ -Al₂O₃.^[27-29,39,40] Especially, HZSM-5 has been considered as an excellent candidate for methanol dehydration.^[31-38] In addition, reaction conditions,^[41-48] catalyst regeneration^[49] and interaction between different functional components^[50] have also been investigated. However, some deficiencies still exist in STD process over the hybrid catalyst. For example, the far distance between active sites of syngas-to-methanol and solid acidic sites leads to the low catalytic performance including activity and selectivity.

Apart from the aforementioned hybrid catalysts, the supported bifunctional catalysts were also frequently used in the STD reactions.^[2,51-60] The supported catalyst can be produced by the coprecipitation, impregnation, sol-gel, and wet-chemical ways.^[61-70] The character and performance of the supported catalysts in the STD reaction strongly depend on their synthesis method. In the last few years, new synthetic technologies such as ultrasound-assisted method and physical sputtering were also employed to prepare the supported bifunctional catalysts.^[71,72] Because the Cu/ZnO-based active sites distribute randomly on the surface of solid-acids, the two tandem reactions (methanol synthesis and the subsequent methanol dehydration) are out of order and take place independently, which results in a low DME selectivity. To address the problem of the open-structure of bifunctional catalysts for direct synthesis of DME from syngas, core-shell capsule catalysts were designed.^[73-83] The selectivity of capsule-structured catalysts obviously is higher

[a] Dr. Yongle Guo, Prof. Zhongkui Zhao
State Key Laboratory of Fine Chemicals, Department of Catalysis
Chemistry and Engineering, School of Chemical Engineering, Dalian
University of Technology, Dalian 116024, P. R. China.
E-mail: zkzhao@dlut.edu.cn

Supporting information for this article is given via a link at the end of the document. ((Please delete this text if not appropriate))

than that of the physically mixed catalysts for DME synthesis owing to their closed capsule-structure. Especially, the capsule-structured CuZnAl@HZSM-5 catalyst by in-situ coating H-ZSM-5 shell over the outside surface of CuZnAl core has been considered as a smart candidate for highly selective synthesis of DME. However, it can hardly avoid the erosion of Cu during the hydrothermal synthesis process of HZSM-5, which leads to much lower CO conversion.^[73] In our research group, we previously reported a facile and robust strategy for preparing a highly efficient CZA-*oa*@H-ZSM-5 capsule-structured bifunctional catalyst by coating an H-ZSM-5 shell on millimeter-sized copper–zinc–aluminum oxalate but not on copper–zinc–aluminum oxide via the hydrothermal crystallization process with the subsequent calcination at 500 °C for 5 h in air. It was found that the direct use of CZA-*oa* to replace CZA could efficiently inhibited Cu leaching in the coating process, besides turning down the necessity of using a rotary oven for the good coating of the H-ZSM-5 shell on the core owing to high hydrophilic property.^[76] In addition, the dual-layer strategies with the formed silicalite-1 zeolite shell as a protection layer was employed for preparation of CuZnAl@H-ZSM-5 capsule catalysts. Unfortunately, the CO conversion also needs to be improved.^[78-80] In order to avoid the damage to the Cu-based core in the process of zeolite coating, a physical coating method as a simple way was developed,^[82,83] in which silica sol was used as a binder for coating zeolite shell. However, the resulting SiO₂ from silica sol inevitably covers the active sites of CuZnAl methanol synthesis catalyst. Moreover, SiO₂ also can block the microporous channels of zeolites. Therefore, it is urgent to search a new binder to prepare core-shell capsule catalyst by the physical coating method.

In this study, capsule-structured CZA@HZSM-5 catalysts were synthesized by using physical coating method with variety viscosities of ethanol, water, methanol, and ethylene glycol as binder to coat micrometer-sized HZSM-5 shell on the prior-shaped millimeter-sized CZA core. The silica sol was also used as binder for comparison. Owing to too low viscosity of methanol, HZSM-5 cannot be attached to the prior shaped CuZnAl microparticles. However, the too large viscosity of ethylene glycol leads to the serious abscission of HZSM-5 from the particles. As a consequence, the HZSM-5 also cannot be attached on the core. Therefore, the liquid binder with appropriate viscosity is required. The CZA@HZSM-5-EtOH catalyst synthesized with ethanol as a binder shows an excellent catalytic performance in syngas-to-DME. It displays 2.9 times higher CO conversion with the 2.7 times higher TOF and 9.2 times higher *STY*_{DME} compared to the CZA@HZSM-5-SS catalyst prepared by using silica sol as a binder (315.5 vs 34.3 g_{DME} kg_{cat}⁻¹ h⁻¹). The effects of types of binder on the nature of capsule-structured CZA@HZSM-5 catalysts and their catalytic performance in dimethyl ether synthesis from syngas were investigated. This work developed a highly-efficient and practical catalyst for syngas-to-dimethyl ether.

The capsule-structured CZA@HZSM-5 catalysts are composed of a millimetre-sized CAZ core as methanol synthesis catalyst and a micrometer-sized HZSM-5 shell as methanol dehydration catalyst. The capsule-structure of the as-prepared

samples is confirmed by SEM and EDS analysis. **Figure 1** demonstrates the surface SEM images and EDS analysis of

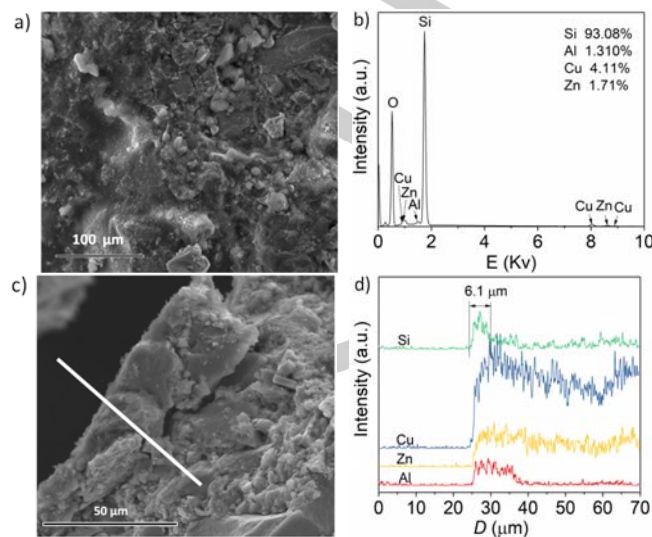


Figure 1. (a) Surface SEM image, (b) surface EDS, (c) cross-section SEM image and (d) EDS line analysis of CZA@HZSM-5-EtOH catalyst.

CZA@HZSM-5-EtOH. From Figure 1a and b, the surface of the CZA@HZSM-5-EtOH is mainly composed of Si while the molar ratio of Cu/Zn/Al/Si is 1.00/0.38/0.19/0.33. This shows the HZSM-5 shell has been covered on the millimeter-sized CZA core. The SEM image and EDS line analysis of cross-section of CZA@HZSM-5-EtOH are shown in Figures 1c and d. The EDS analysis is collected along the white line in the SEM image. It displays the alteration of elemental signals from the HZSM-5 shell to the CZA core part. Figure 1d shows that the Si signal sharply increases in the HZSM-5 shell and then reduces at the interface between HZSM-5 layer and millimetre-sized CZA core, displaying the HZSM-5 shell with about 6.1 µm thickness coating on core. **Figures 2a** and **b** exhibit the surface SEM images and EDS analysis of CZA@HZSM-5-SS. The signals of Si and Al on the surface of CZA@HZSM-5-SS are the overwhelming majority, and the signal of Cu and Zn on the outer surface of samples are very low, indicating successful coating of HZSM-5 zeolite by using silica sol as a binder. The **Figures 2c** and **d** show SEM images and EDS line analysis of cross-section of CZA@HZSM-5-SS. The EDS analysis displays the alteration of element signal from the HZSM-5 zeolite to the CZA core part. What is worth noting is that there are two sharp Si signs in Figure 2d. It shows that the Si signal increased sharply in the HZSM-5 zeolite shell and then gradually decreased at the interface between HZSM-5 zeolite shell and the formed SiO₂ from silica sol, indicating the existence of zeolite shell with 5.4 µm of thickness and the middle SiO₂ layer with 4.4 µm of thickness. Moreover, from Figure S1, the HZSM-5 zeolite shell is also successfully covered on the millimetre-sized CZA core by using water as a binder. The thickness of zeolites shell is 3.6 µm, which is thinner than that of CZA@HZSM-5-EtOH and CZA@HZSM-5-SS. The above results

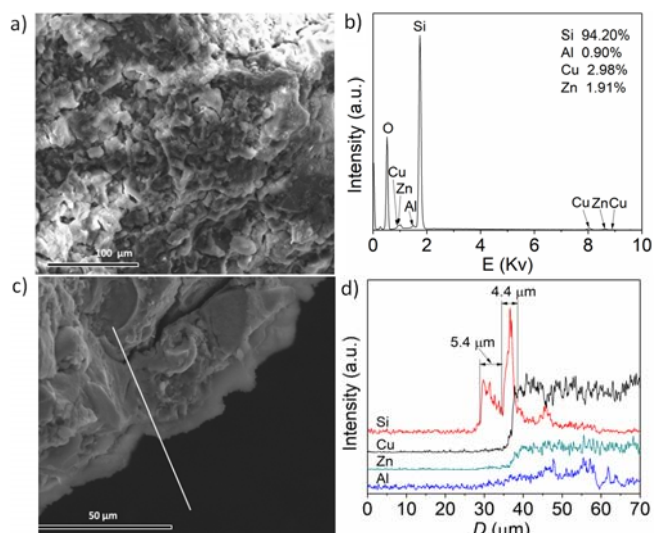


Figure 2. (a) Surface SEM image, (b) surface EDS analysis, (c) cross-section SEM image and (d) EDS line analysis of CZA@HZSM-5-SS catalyst.

demonstrate that HZSM-5 shell can be successfully coated on the millimeter-sized CZA core by using ethanol, water or silica sol as a binder. However, when silica sol is used to binder, the resulting SiO₂ layer between millimeter-sized CZA core and HZSM-5 shell cannot be avoided. From Table 1, the decrease in the exposed Cu active sites of the core-shell catalysts compared to the CZA core can present a further evidence for the successfully coating HZSM-5 shell on the CZA core. Moreover, compared to the CZ@HZSM-5-EtOH catalyst without Al in the core, the CZA@HZSM-5-EtOH catalyst show higher exposed Cu active sites. This suggests the promoting Cu dispersion in the CZA@HZSM-5-EtOH catalyst by the Al in the core.

The XRD patterns of core CZA catalyst, CZA@HZSM-5-EtOH and CZA@HZSM-5-SS capsule catalysts are showed in **Figure 3**. The peaks in the ranges of 5~10° and 21~25° of

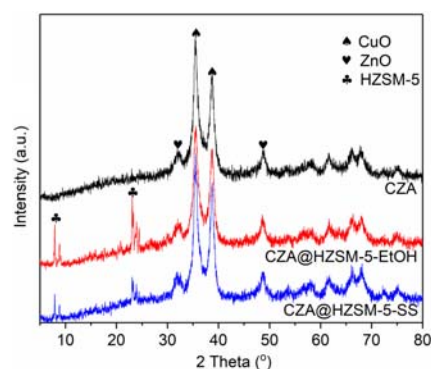


Figure 3. XRD patterns of CZA, CZA@HZSM-5-EtOH and CZA@HZSM-5-SS.

CZA@HZSM-5-EtOH and CZA@HZSM-5-SS belong to HZSM-5. As it is shown in the Figure 3 and S2, the diffraction patterns corresponding to CuO and ZnO on the capsule-structured CZA@HZSM-5-EtOH, CZA@HZSM-5-SS and CZA@HZSM-5-

H₂O catalysts are consistent with those of CZA, which shows that the damage towards CZA core by the physical coating process.

Nitrogen adsorption is conducted to investigate the textural properties of catalysts. The adsorption-desorption isotherms and pore size distribution of CZA, CZA@HZSM-5-EtOH and CZA@HZSM-5-SS catalysts are shown in **Figure 4**. From Figure 4, the pores with a size of 5-25 nm in the catalysts can be

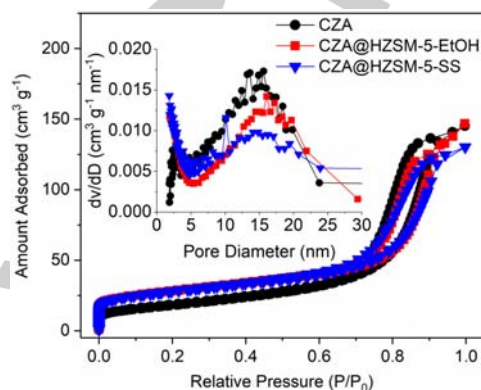


Figure 4. Nitrogen adsorption-desorption isotherms and pore size distributions from adsorption branch of, CZA, CZA@HZSM-5-EtOH and CZA@HZSM-5-SS.

assigned to the intercrystalline pores. The coating of zeolite shell on the millimeter-sized core CZA catalyst leads to a reduced amount of the intercrystalline pores of CZA, which may be due to the filling and/or of coverage of pores by HZSM-5. Furthermore, from **Table 1**, the mesoporous volumes of

Table 1. Characterization data of the CZA core and the capsule-structured CZA@HZSM-5-EtOH and CZA@HZSM-5-SS catalysts.

Catalyst	$S_{\text{BET}}^{\text{[a]}}$ [m ² g ⁻¹]	$S_{\text{t-plot}}^{\text{[b]}}$ [m ² g ⁻¹]	$V_{\text{meso}}^{\text{[c]}}$ [ml g ⁻¹]	$n_{\text{Cu}}^{\text{[d]}}$ [μmol g ⁻¹]	$n_{\text{acid}}^{\text{[e]}}$ [μmol g ⁻¹]	$n_{\text{H}_2}^{\text{[f]}}$ [mmol g ⁻¹]
CZA	64.8	0	0.22	422.1	-	2.3
CZA@HZSM-5-SS	97.6	35.4	0.19	362.9	112.9	1.9
CZA@HZSM-5-EtOH	97.7	37.4	0.21	389.3	133.5	2.0
CZ@HZSM-5-EtOH	-	-	-	157.4	63.0	2.2

[a] BET specific surface area from N₂ adsorption-desorption experiments. [b] t-plot method. [c] $V_{\text{meso}} = V_{\text{total}} - V_{\text{t-plot}}$. [d] Amount of surface active Cu, determined by H₂-TPR after oxidation of the samples by N₂O. [e] Measured by NH₃-TPD. [f] Determined by H₂-TPR.

CZA@HZSM-5-EtOH and CZA@HZSM-5-SS are 0.21 ml g⁻¹ and 0.19 ml g⁻¹, respectively, which are lower than that of CZA (0.22 ml g⁻¹). Besides, the degree of blocking of CZA@HZSM-5-SS is more serious than that of CZA@HZSM-5-EtOH. From Figures 4 and S3, the sharp increase in amount of adsorbed N₂ at the low P/P₀ on the isotherms of the three core-shell CZA@HZSM-5 catalysts, indicating the existence of micropores. From Table 1 and S1, CZA@HZSM-5-EtOH, CZA@HZSM-5-SS and CZA@HZSM-5-H₂O have 37.4, 35.4, and 26.3 m² g⁻¹ of microporous surface area, respectively. This is an evidence for the successfully coating HZSM-5 on the millimetre-sized CZA

cores by using the different binders in the physical coating process.

H₂-temperature-programmed reduction was conducted to investigate the impact of binder type on the reduction behavior of various capsule-structured CZA@HZSM-5 catalysts. From Figure S4, there exist two kinds of reduction peaks for all samples, which can be assigned to surface and bulk reducible Cu species in the core.^[4] The changes in reduction peaks of the coating CZA catalysts compared to the bare CZA might be led by the coating process. Moreover, the redox behavior of CZA@HZSM-5-EtOH catalyst and CZ@HZSM-5-EtOH catalyst without Al in the core was compared. The CZ@HZSM-5-EtOH catalyst shows higher reduction temperature than CZA@HZSM-5-EtOH, implying the promoting effect of Al in the core on the Cu dispersion. The promoted Cu dispersion of CZA@HZSM-5-EtOH compared to CZ@HZSM-5-EtOH can also be confirmed by its more exposed Cu active sites listed in Table 1.

Figure S5 shows the NH₃-TPD profiles of the capsule-structured CZA@HZSM-5 catalysts. It is observed that weak acid sites (150 - 300 °C) and medium acid sites (300 - 450 °C) exist in these core-shell CZA@HZSM-5 capsule catalysts. Weak and medium acid sites are identified as the ideal acid active sites for methanol dehydration to dimethyl ether.^[2] From Table 1 and S1, CZA@HZSM-5-EtOH shows more the acidic sites (133.5 μmol g⁻¹) than CZA@HZSM-5-H₂O (115.3 μmol g⁻¹) and CZA@HZSM-5-SS (112.9 μmol g⁻¹), which can promote the conversion of the as-formed methanol on the cores into DME. Moreover, the existence of Al in the core increases the acidic amounts of CZA@HZSM-5-EtOH catalyst compared to the CZ@HZSM-5-EtOH catalyst without Al in the core.

The STD reaction is a tandem reaction, which includes the methanol synthesis process from syngas over the Cu-based catalysts and methanol dehydration to DME over the solid acid. The STD process was carried out using the core-shell capsule catalyst composed of millimeter-sized CZA core and micrometer-sized HZSM-5 shell, which is thermodynamically beneficial and more efficient than the conventional DME synthesis by two separated processes.^[73-83] The catalytic performances of the CZA@HZSM-5-EtOH, CZA@HZSM-5-H₂O and CZA@HZSM-5-SS are shown in the **Table 2** and S2. The TOF was calculated

Table 2. Catalytic performance of the CZA@HZSM-5-EtOH and CZA@HZSM-5-SS catalysts for dimethyl ether direct synthesis from syngas.^[a]

Catalyst	CO Con. [mol %]	TOF [min ⁻¹]	CO-to-CO ₂ [mol %]	Product distribution [Carbon mol %]		
				MeOH	DME	CH ₄
CZA@HZSM-5-SS	26.3	0.3	2.8	72.7	25.8	1.5
CZA@HZSM-5-EtOH	76.5	0.8	17.7	4.8	95.0	0.2
CZ@HZSM-5-EtOH	9.8	0.3	1.9	7.3	89.6	3.1

[a] Reaction condition: 0.5 g catalyst, *P* = 3.0 MPa, *T* = 250 °C, H₂/CO/N₂ = 10/5/5, *GHSV* = 1800 ml g⁻¹ h⁻¹, 5 h of TOS.

based on the amount of exposed Cu active sites per gram catalyst listed in Table 1. It can be seen that CZA@HZSM-5-EtOH and CZA@HZSM-5-H₂O show 76.5% and 61.0% of high CO conversion, respectively, which are 2.9 times and 2.3 times

higher than that over CZA@HZSM-5-SS (26.3 %) under the same reaction conditions. The high DME distributions (based on the total hydrocarbons and oxygenates formed without CO₂) of CZA@HZSM-5-EtOH and CZA@HZSM-5-H₂O are 95.0 % and 88.0%, respectively. However, the value of DME selectivity over the CZA@HZSM-5-SS catalyst is only 25.8%, and the methanol is the main production. It is worth to note that, from the above analysis, HZSM-5 is successfully covered on the outer surface of millimetre-sized core CZA catalyst when using silica sol as binder. In addition, the amounts of the acidic sites over the CZA@HZSM-5-SS are similar as that over the CZA@HZSM-5-H₂O. However, the DME selectivity over the CZA@HZSM-5-H₂O is further higher than that of CZA@HZSM-5-SS catalyst. The reason why the selectivity of DME over the CZA@HZSM-5-SS is so low is the SiO₂ layer between the millimetre-size core CZA and HZSM-5 zeolites. It can be seen from Figure 2c and d that the SiO₂ layer nearly capped on the outer surface of millimetre-sized CZA core catalyst and was covered by the HZSM-5 zeolites. The schematics of methanol dehydration over the (a) CZA@HZSM-5-EtOH and CZA@HZSM-5-H₂O, and (b) CZA@HZSM-5-SS catalyst were drawn in **Figure 5**. When

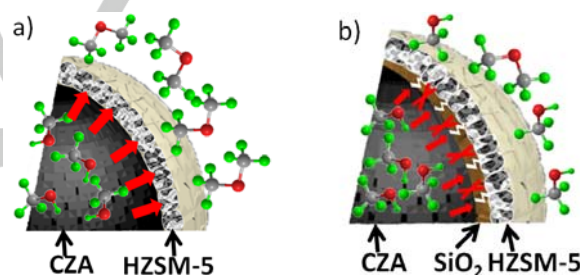


Figure 5. Schematic of methanol dehydration to DME over the (a) CZA@HZSM-5-EtOH and CZA@HZSM-5-H₂O, (b) CZA@HZSM-5-SS.

ethanol and water are used as binder, the HZSM-5 nearly clings on the outer surface of millimetre-sized CZA core, so the methanol molecules formed over the CZA core can entirely pass through the micropores of HZSM-5 and dehydrate on the acidic sites. However, owing to the existence of SiO₂ layer in the CZA@HZSM-5-SS catalyst, the formed methanol molecules over the CZA core can't directly enter into the micropore of HZSM-5 to access to the acidic sites. As a result, CZA@HZSM-5-SS shows much lower DME selectivity than the developed CZA@HZSM-5-EtOH by using EtOH as a binder. Furthermore, the compressed methanol dehydration of methanol over the CZA@HZSM-5-SS catalyst depresses the CO conversion since the methanol synthesis from syngas is a thermodynamic equilibrium limited reaction. As a result, CZA@HZSM-5-EtOH catalyst shows both higher CO conversion and DME selectivity than the other catalysts. Moreover, owing to the promoting effect of improved methanol dehydration, CZA@HZSM-5-EtOH catalyst shows much higher TOF than others. Furthermore, as in shown in the previous report,^[73] Al migration from CuZnAlO core to Silicalite-1 membrane is a key factor to get H-ZSM-5 membrane finally. Encouraged by the result, we explored what

would happen when CuZnO is the core of catalyst in the absence of Al (CZ@HZSM-5-EtOH). From Table 2, CZ@HZSM-5-EtOH shows unexpectedly lower CO conversion (9.8% vs. 76.5%) and TOF (0.3 vs. 0.8) than CZA@HZSM-5-EtOH. From Table 1, the much higher exposed Cu on CZA@HZSM-5-EtOH catalyst by Al promoted Cu dispersion than that on CZ@HZSM-5-EtOH leads to its higher CO conversion. For another, the presence of Al in the CZA core of CZA@HZSM-5-EtOH catalyst can strengthen the CO adsorption,^[85] which can also promote CO hydrogenation. Moreover, Al in the core of CZA@HZSM-5-EtOH catalyst also endows it with some extra acidic sites.^[76] As a result, CZA@HZSM-5-EtOH catalyst shows much more acidic sites than CZ@HZSM-5-EtOH (Table 1), and then the former shows lower methanol content than the latter (4.8% vs. 7.3%). Furthermore, CZA@HZSM-5-EtOH catalyst shows lower methane (0.2% vs. 3.1%) contents than CZ@HZSM-5-EtOH, which might be ascribed to the resulted change in the redox behaviour of CZA@HZSM-5-EtOH by the Al in the core of the catalyst, compared to the CZ@HZSM-5-EtOH without Al in the core.

Moreover, the space time yield of DME over the diverse capsule-structured catalysts prepared with various binders and the catalytic stability of the optimized CZ@HZSM-5-EtOH catalyst were investigated. From Figure 6a, the space time yield

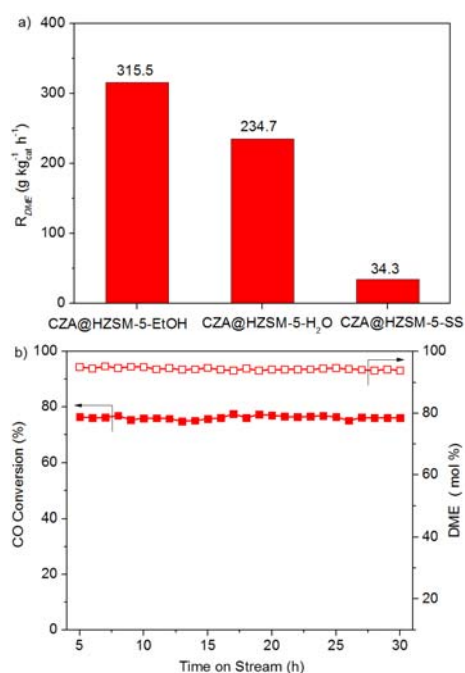


Figure 6. a) The space time yield of DME over CZA@HZSM-5-EtOH, CZA@HZSM-5-H₂O and CZA@HZSM-5-SS. b) Catalytic stability of the developed CZA@HZSM-5-EtOH for dimethyl ether direct synthesis from syngas.

of DME over CZA@HZSM-5-EtOH is $315.5 \text{ g}_{\text{DME}} \text{ kg}_{\text{cat}}^{-1} \text{ h}^{-1}$, which is much higher than those over the CZA@HZSM-5-H₂O ($234.7 \text{ g}_{\text{DME}} \text{ kg}_{\text{cat}}^{-1} \text{ h}^{-1}$) and CZA@HZSM-5-SS ($34.3 \text{ g}_{\text{DME}} \text{ kg}_{\text{cat}}^{-1} \text{ h}^{-1}$)

¹) catalyst. From Table S4, in contrast to the previously reported syngas-to-DME catalysts, the capsule-structured CZA@HZSM-5-EtOH catalyst indicates much higher DME STY_{DME} under similar conditions of $GHSV$. From the above results, we developed an efficient syngas-to-dimethyl ether core-shell bifunctional CZA@HZSM-5-EtOH catalyst with 1.00/0.38/0.19/0.33 of Cu/Zn/Al/Si molar ratio (by XRF). The CZA@HZSM-5-EtOH catalyst has a similar Cu/Zn ratio to the CZA core, suggesting the physical coating process of HZSM-5 shell with ethanol as a binder doesn't have visible influence on the CZA core. This endows CZA@HZSM-5-EtOH catalyst with outstanding catalytic performance concerning activity and selectivity in direct synthesis of DME from syngas. The stability of CZA@HZSM-5-EtOH for DME synthesis from syngas was illustrated in Figure 6b. From Figure 6b, the developed CZA@HZSM-5-EtOH catalyst by a facile physical coating method with EtOH as a binder shows excellent catalytic stability. No visible decrease in either CO conversion or DME selectivity along with 30 h of time of stream can be observed. In a word, we develop a highly-efficient and practical capsule-structured catalyst by a physical coating approach using ethanol as a binder, which shows excellent catalytic performance for direct synthesis of dimethyl ether from syngas.

In summary, a capsule-structured CZA@HZSM-5-EtOH catalyst was prepared by a physical coating method with ethanol as a binder through coating prior-shaped millimeter-sized CZA core with micrometer-sized HZSM-5 shell, which shows outstanding catalytic performance for direct synthesis of dimethyl ether from syngas. The developed CZA@HZSM-5-EtOH exhibits 2.9 times higher CO conversion with 2.7 times higher turnover frequency and 9.2 times higher dimethyl ether space-time yield than the previously reported CZA@HZSM-5-SS catalyst with silica sol as a binder. The much superior catalytic performance of CZA@HZSM-5-EtOH to CZA@HZSM-5-SS can be ascribed to the elimination of block effect of silica through replacing silica sol by ethanol on the access of the reactant to copper active sites and the synthesized methanol to acidic sites of HZSM-5 shell. This work not only produces an outstanding CO-to-DME catalyst, but also develops a new method for designing highly-efficient core-shell catalysts by a physical coating method.

Experimental Section

Materials: Copper nitrate trihydrate (Tianjin Damao Chemical Reagent Co. AR), zinc nitrate hexahydrate (Aladdin, AR), aluminum nitrate nonahydrate (Sinopharm Chemical Reagent Co., Ltd, AR), ethanol solution (Tianjin Tianda Chemical Reagent Co. AR), oxalate (Tianjin Tianda Chemical Reagent Co. AR), tetraethyl orthosilicate (TEOS, Xilong Scientific Reagent Co. AR), tetrapropylammonium hydroxide (TPAOH, 25 wt.% Sinopharm Chemical Reagent Co., Ltd, AR), aluminium isopropoxide (Aladdin, AR), silica sol (Ludox: 30 wt. %, Shandong Usoff Chemical Technology Co.).

Catalyst preparation: The core CuO/ZnO/Al₂O₃ (CZA) catalyst was synthesized by oxalate co-precipitation method at room temperature with subsequent calcination and shaping.^[73] Firstly, 45 mmol of copper nitrate trihydrate, 20 mmol of zinc nitrate hexahydrate and 10 mmol of aluminum

nitrate nonahydrate were dissolved in 75 ml of ethanol solution. Then 90 mmol of oxalate was added into 90 ml of ethanol solution. Above two ethanol solutions was mixed and follow by stirring for 4h at room temperature. The colloid was separated by centrifugal process. The obtained samples was dried at 105 °C and calcined at 370 °C for 1h. The powder of $\text{CuO}/\text{ZnO}/\text{Al}_2\text{O}_3$ was squeezed and sieved into granules with 20-40 mesh. HZSM-5 was synthesized as the follow method:^[84] the molar composition ratio of the synthesis compounds was 1TEOS:0.00625 Al_2O_3 :0.27TPAOH:57.69 H_2O . After the mixture was stirred for 2 h at 35 °C, the precursor of HSM-5 was treated at 80 °C in order to remove the ethanol produced during the hydrolysis of TEOS. Then the water was added to keep a constant volume. Crystallization process was conducted at 180 °C for 72 h, the product was collected by centrifugation, dried and calcination in static air at 540 °C for 6 h. The CZA@HZSM-5-EtOH capsule catalyst is synthesized by physical coating method as given in the following: 0.2 g of HZSM-5 powder was added into 5 ml of ethanol solution in a 20 ml beaker and stirred by glass bar for uniform disperse of HZSM-5. Then 1.0 g of CZA granules was added into the liquid mixture and immersed at 2h. Then, the mixture was turned into oven and dried at 40 °C. In this process, the capsule catalyst was vigorously sharked and stirred carefully with a glass bar every 20 min in order to obtain a uniform HZSM-5 shell on the out of CZA catalyst. When water as a binder, the preparation of sample is similar with CZA@HZSM-5-EtOH, apart from the ethanol was replaced by water and dried at 60 °C. It is noted by CZA@HZSM-5- H_2O . As silica sol is binder, the sample is indicated by signed CZA@HZSM-5-SS. For comparison, CZA@HZSM-5-SS was prepared according to the reference.^[82] Typically, 0.33 g of silica sol was diluted with 2 times water in weight. The 1.0 g of CZA granules was added into the diluted silica sol and was immersed. Then, the HZSM-5 powder was mixed with the soaked $\text{CuO}/\text{ZnO}/\text{Al}_2\text{O}_3$ catalyst in a break, follow by vigorously shaking and stirring. Then, the sample was turned into oven and dried at 60 °C. In this process, the capsule catalyst was vigorously sharked and stirred carefully with a glass bar every 20 min. Finally, dried samples were treated by calcinations at 500 °C for 2 h at heating rate 5 °C min^{-1} .

Catalyst characterization: The surface architecture of the catalysts and distribution of element of catalysts cross-section were investigated by scanning electron microscope (SEM) and energy dispersive spectrometer (EDS) on FEI QUANTA 450 SEM/EDX instrument. N_2 adsorption-desorption experiments were conducted using a Beishide 3H-2000PS1 apparatus at -196 °C. The specific surface areas and micropores areas of the samples were calculated by BET method and t -plot method, respectively. The mesoporous volume was defined as total volume reduced microporous volume. X-ray diffraction (XRD) patterns of the catalysts were collected in the 2θ range of 5°–80° with a speed of 8° min^{-1} on a Rigaku D/max-2400 instrument. H_2 -temperature-programmed reduction (H_2 -TPR) measurements were carried out on a Builder Chemisorption (PCA-1200) instrument equipped a thermal conductivity detector (TCD). The sample (50 mg) was placed in a U-shape quartz tube and treated at 250 °C for 1h in the flowing Ar, and then cooled down to 50 °C. After that, gas flow was switched to 10 % H_2/Ar at 50 mL min^{-1} , the catalyst was reduced at 400 °C by a heating rate of 5 °C min^{-1} . The numbers of H_2 consumption were gained by integrating and transforming the TPR peak area. The quantities of superficial Cu atoms of samples were investigated by H_2 -TPR after samples oxidized by N_2O at 50 °C. The procedure was as follows: 50 mg of samples were reduced in flowing 10 % H_2/Ar (30 ml min^{-1}) at 250 °C for 2 h, and then cooled down to 50 °C. After being purified with He for 30 min, the metallic copper were oxidized by 10 % $\text{N}_2\text{O}/\text{He}$ (30 ml min^{-1}) at 50 °C for 1 h. Next, in order to remove the residual N_2O , the samples were purified with Ar for 30 min. Finally, the 10 % H_2/Ar (30 ml min^{-1}) was introduced through the sample and the samples were reduced at 400 °C by a heating rate of 10 °C min^{-1} . The quantities of surface Cu molecules are twice the quantity of

consumptive H_2 molecules. NH_3 temperature-programmed desorption (NH_3 -TPD) experiment was conducted on a Builder Chemisorption (PCA-1200) instrument with a TCD. The 100 mg of sample was firstly pretreated in the flowing Ar at 500 °C for 60 min, and then cooled to below 100 °C. The ammonia adsorption process was performed at 100 °C via pulse injection of ammonia. NH_3 desorption process was conducted by heating the sample from 100 to 500 °C with a heating rate of 10 °C min^{-1} in the flowing Ar.

Catalytic performance test: Syngas-to-dimethyl ether reaction was performed in fixed-bed with a stainless steel reactor (8 mm) at 3.0 Mpa and 250 °C. Firstly, 0.5 g of sample was reduced at atmospheric pressure in the flowing gas (10 ml min^{-1} H_2 with 20 ml min^{-1} N_2) at 250 °C for 2h. Then STD reactions were carried out under the conditions: 250 °C, 3.0 Mpa, GHSV is 1800 ml g^{-1} h^{-1} , and feed gas ($\text{H}_2/\text{CO}/\text{N}_2 = 10/5/5$ molar ratio). The effluent products were heated at 160 °C and analyzed by an online gas chromatograph (FULI 9790 II) that was equipped with Porapak N and 5A molecular sieve packed columns. The carbon balance of the reaction over the CZA@HZSM-5-EtOH, CZA@HZSM-5- H_2O and CZA@HZSM-5-SS catalysts are 101.4%, 99.4% and 99.3%, respectively. The internal standard method was used to calculate the CO conversion and organic product distribution by the Eq. 1 and 2, respectively:

$$\text{CO conversion (mol \%)} = \left(1 - \frac{\text{CO}_{\text{out}}}{\text{CO}_{\text{in}}}\right) \times 100 \% \quad (\text{Eq. 1})$$

$$\text{C}^i \text{ distribution (mol \%)} = \frac{\text{Mole of C}^i \text{xi}}{\sum_{i=1}^n \text{Mole of C}^i \text{xi}} \times 100 \% \quad (\text{Eq. 2})$$

Where CO_{in} and CO_{out} stands for the molar fraction of CO at the inlet and outlet, respectively. C^i represent the organic product of CH_3OH , CH_4 , DME, and i is for the carbon number in the molecules.

The formed CO_2 was assessed by the CO conversion to CO_2 (mol %). In addition, the turnover frequency (TOF) of CO was calculated as the converted CO per min per surfacial Cu atom. The space time yield of DME (STY_{DME}) was calculated as the gram of as-formed DME per h per g catalyst. They were calculated employing equations 3 and 4, respectively:

$$\text{TOF (min}^{-1}\text{)} = \frac{F_{\text{CO}} \times \text{COconv.}}{1000 \times V_{\text{M}} \times n_{\text{Cu}}} \quad (\text{Eq. 3})$$

$$\text{STY}_{\text{DME}} = \frac{n_{\text{DME}} \times M_{\text{DME}}}{W_{\text{cat}}} \quad (\text{Eq. 4})$$

Where the F_{CO} is defined as the CO flow rate (ml min^{-1}), V_{m} is the molar volume of an ideal gas at 298 K (24.5 L mol^{-1}), n_{Cu} is the mole of surface Cu atom of the loaded catalyst for the catalysis test, and the n_{DME} is defined as the as-formed DME mol per h, M_{DME} is the molecular mass of DME, and W_{cat} is the mass of catalyst.

Acknowledgements

This work was financially supported by the National Natural Science Foundation of China (U1610104) and also by the Chinese Ministry of Education via the Program for New Century Excellent Talents in Universities (NCET-12-0079).

Keywords: capsule-structured catalyst • physical coating • ethanol as a binder • H-ZSM-5 • $\text{Cu}/\text{ZnO}/\text{Al}_2\text{O}_3$ • syngas to dimethyl ether

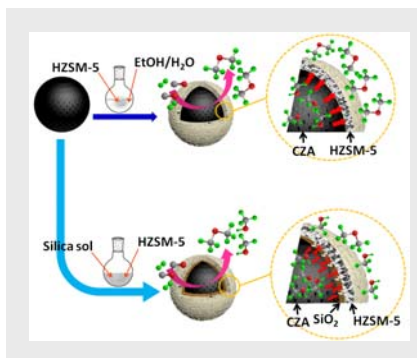
- [1] W. Zhou, K. Cheng, J. Kang, C. Zhou, V. Subramanian, Q. Zhang, Y. Wang, *Chem. Soc. Rev.* **2019**, *48*, 3193–3228.
- [2] J. Sun, G. Yang, Y. Yoneyama, N. Tsubaki, *ACS Catal.* **2014**, *4*, 3346–3356.
- [3] J. J. Lewnard, T. H. Hsiung, J. F. White, and D. M. Brown, *Chem. Eng. Sci.* **1990**, *45*, 2735–2741.
- [4] J. L. Li, X. G. Zhang, T. Inui, *Appl. Catal. A: Gen.* **1996**, *147*, 23–33
- [5] S. Kuld, M. Thorhauge, H. Falsig, C. F. Elkjær, S. Helveg, I. Chorkendorff, J. Sehested, *Science* **2016**, *352*, 969–974.
- [6] S. A. Kondrat, P. J. Smith, P. P. Wells, P. A. Chater, J. H. Carter, D. J. Morgan, E. M. Fiordaliso, J. B. Wagner, T. E. Davies, L. Lu, J. K. Bartley, S. H. Taylor, M. S. Spencer, C. J. Kiely, G. J. Kelly, C. W. Park, M. J. Rosseinsky, G. J. Hutchings, *Nature* **2016**, *531*, 83–87.
- [7] Y. Wei, P. E. De Jongh, M. L.M. Bonati, D. J. Law, G. J. Sunley, K. P. De Jong, *Appl. Catal. A: Gen.* **2015**, *504*, 211–219.
- [8] D. Masih, S. Rohani, J. N. Kondo, T. Tatsumi, *Appl. Catal. B: Environ.* **2017**, *217*, 247–255.
- [9] H. An, F. Zhang, Z. Guan, X. Liu, F. Fan, C. Li, *ACS Catal.* **2018**, *8*, 9207–9215.
- [10] C. Zhou, N. Wang, Y. Qian, X. Liu, J. Caro, A. Huang, *Angew. Chem. Int. Ed.* **2016**, *55*, 12678–12682.
- [11] A. Ghorbanpour, J. D. Rimer, L.C. Grabow, *ACS Catal.* **2016**, *6*, 2287–2298.
- [12] S. Müller, Y. Liu, F. M. Kirchberger, M. Tonigold, M. Sanchez-sanchez, J. A. Lercher, *J. Am. Chem. Soc.* **2016**, *138*, 15994–16003.
- [13] F. Yaripour, F. Baghaei, I. Schmidt, J. Perregaard, *Catal. Commun.* **2005**, *6*, 147–152.
- [14] S. S. Akarmazyan, P. Panagiotopoulou, A. Kambolis, C. Papadopoulou, D. I. Kondarides, *Appl. Catal. B: Environ.* **2014**, *145*, 136–148.
- [15] D. Liu, C. Yao, J. Zhang, D. Fang, D. Chen, *Fuel* **2011**, *90*, 1738–1742.
- [16] R. M. Ladera, J. L. G. Fierro, M. Ojeda, S. Rojas, *J. Catal.* **2014**, *312*, 195–203.
- [17] W. Alharbi, E. F. Kozhevnikova, I. V. Kozhevnikov, *ACS Catal.* **2015**, *5*, 7186–7193.
- [18] G. S. Foo, G. Hu, Z. D. Hood, M. Li, D. E. Jiang, Z. Wu, *ACS Catal.* **2017**, *7*, 5345–5356.
- [19] M. Xu, J. H. Lunsford, D. W. Goodman, A. Bhattacharyya, *Appl. Catal. A: Gen.* **1997**, *149*, 289–301.
- [20] V. Vishwanathan, H. -S. Roh, J. W. Kim, K. W. Jun, *Catal. Lett.* **2004**, *96*, 23–28.
- [21] Y. Hua, X. Guo, D. Mao, G. Lu, G. L. Rempel, F. T. T. Ng, *Appl. Catal. A: Gen.* **2017**, *540*, 68–74.
- [22] X. Zhou, T. Su, Y. Jiang, Z. Qin, H. Ji, Z. Guo, *Chem. Eng. Sci.* **2016**, *153*, 10–20.
- [23] R. Liu, Z. Qin, H. Ji, T. Su, *Ind. Eng. Chem. Res.* **2013**, *52*, 16648–16655.
- [24] M. Cai, V. Subramanian, V. V. Sushkevich, V. V. Ordonsky, A. Y. Khodakov, *Appl. Catal. A: Gen.* **2015**, *502*, 370–379.
- [25] F. Arena, K. Barbera, G. Italiano, G. Bonura, L. Spadaro, F. Frusteri, *J. Catal.* **2007**, *249*, 185–194.
- [26] A. Garcia-Trenco, A. Martínez, *Appl. Catal. A: Gen.* **2015**, *493*, 40–49.
- [27] S. Asthana, C. Samanta, R.K. Voolapalli, B. Saha, *J. Mater. Chem. A* **2017**, *5*, 2649–2663.
- [28] M. Gentzen, W. Habicht, D. E. Doronkin, J. D. Grunwaldt, J. Sauer, S. Behrens, *Catal. Sci. Technol.* **2015**, *6*, 1054–1063.
- [29] A. G. Trenco, E. R. White, M. S. P. Shaffer, C. K. Williams, *Catal. Sci. Technol.* **2016**, *6*, 4389–4397.
- [30] V. M. Lebarbier, R. A. Dagle, L. Kovarik, J. A. L. Adarme, D. L. King, D. . Palo, *Catal. Sci. Technol.* **2012**, *2*, 2116–2127.
- [31] M. Cai, A. Palčić, V. Subramanian, S. Moldovan, O. Ersen, V. Valtchev, V. V. Ordonsky, A. Y. Khodakov, *J. Catal.* **2016**, *338*, 227–238.
- [32] R. Montesano, A. Narvaez, D. Chadwick, *Appl. Catal. A: Gen.* **2014**, *482*, 69–77.
- [33] Y. Wang, W. L. Wang, Y. Chen, J. Zheng, R. Li, *J. Fuel Chem. Technol.* **2013**, *41*, 873–880.
- [34] A. G. Trenco, S. Valencia, A. Martínez, *Appl. Catal. A: Gen.* **2013**, *468*, 102–111.
- [35] A. G. Trenco, A. Martínez, *Appl. Catal. A: Gen.* **2012**, *411–412*, 170–179.
- [36] D. Mao, W. Yang, J. Xia, B. Zhang, Q. Song, Q. Chen, *J. Catal.* **2005**, *230*, 140–149.
- [37] J. A. Dahrieh, D. Rooney, A. Goguet, Y. Saih, *Chem. Eng. J.* **2012**, *203*, 201–211.
- [38] V. V. Ordonsky, M. Cai, V. Sushkevich, S. Moldovan, O. Ersen, C. Lancelot, V. Valtchev, A. Y. Khodakov, *Appl. Catal. A: Gen.* **2014**, *486*, 266–275.
- [39] S. H. Lima, A. M. S. Forrester, L. A. Palacio, A. C. Faro, *Appl. Catal. A: Gen.* **2014**, *488*, 19–27.
- [40] D. Mao, W. Yang, J. Xia, B. Zhang, G. Lu, *J. Mol. Catal. A: Chem.* **2006**, *250*, 138–144.
- [41] D. Iranshahi, R. Saeedi, K. Azizi, *Fuel* **2017**, *190*, 386–395.
- [42] H. Chen, C. Fan, C. Yu, *Appl. Energy* **2013**, *101*, 449–456.
- [43] M. Jia, W. Li, H. Xu, S. Hou, Q. Ge, *Appl. Catal. A: Gen.* **2002**, *233*, 7–12.
- [44] E. Peral, M. Martín, *Ind. Eng. Chem. Res.* **2015**, *54*, 7465–7475.
- [45] A. Bayat, T. Dogu, *Ind. Eng. Chem. Res.* **2016**, *55*, 11431–11439.
- [46] W. Ding, M. Klumpp, H. Li, U. Schygulla, P. Pfeifer, W. Schwieger, K. Haas-Santo, R. Dittmeyer, *J. Phys. Chem. C* **2015**, *119*, 23478–23485.
- [47] G. Moradi, J. Ahmadpour, M. Nazari, F. Yaripour, *Ind. Eng. Chem. Res.* **2008**, *47*, 7672–7679.
- [48] I. Sierra, J. Ereña, A. T. Aguayo, J. M. Arandes, M. Olazar, J. Bilbao, *Appl. Catal. B: Environ.* **2011**, *106*, 167–173.
- [49] I. Sierra, J. Ereña, A. T. Aguayo, J. M. Arandes, J. Bilbao, *Appl. Catal. B: Environ.* **2010**, *94*, 108–116.
- [50] A. G. Trenco, A. V. Moya, A. Martínez, *Catal. Today* **2012**, *179*, 43–51.
- [51] A. Atakan, E. Erdtman, P. Mäkie, L. Ojamäe, M. Odén, *J. Catal.* **2018**, *362*, 55–64.
- [52] M. Stiefel, R. Ahmad, U. Arnold, M. Döring, *Fuel Pro. Tech.* **2011**, *92*, 1466–1474.
- [53] Q. Zhang, Y. Z. Zuo, M. H. Han, J. F. Wang, Y. Jin, F. Wei, *Catal. Today* **2010**, *150*, 55–60.
- [54] F. Frusteri, M. Cordaro, C. Cannilla, G. Bonura, *Appl. Catal. B: Environ.* **2015**, *162*, 57–65.
- [55] H. Jiang, H. Bongard, W. Schmidt, F. i Schüth, *Micro. Meso. Mater.* **2012**, *164*, 3–8.
- [56] Y. Wang, Y. Chen, F. Yu, D. Pan, B. Fan, J. Ma, R. Li, *J. Energy Chem.* **2016**, *25*, 775–781.
- [57] R. Ahmad, D. Schrempf, S. Behrens, J. Sauer, M. Döring, U. Arnold, *Fuel Proce. Tech.* **2014**, *121*, 38–46.
- [58] H. J. Kim, H. Jung and K. Y. Lee, *Korean J. Chem. Eng.* **2001**, *18*, 838–841.
- [59] V. M. Lebarbier, R. A. Dagle, L. Kovarik, J. A. L. Adarme, D. L. King and D. R. Palo, *Catal. Sci. Technol.* **2012**, *2*, 2116–2127.
- [60] S. H. Kang, J. W. Bae, H. S. Kim, G. M. Dhar, and K. W. Jun, *Energy Fuels* **2010**, *24*, 804–810.
- [61] G. R. Moradi, S. Nosrati, F. Yaripour, *Catal. Commun.* **2007**, *8*, 598–606.
- [62] Y. Luan, *Adv. Mater. Res.* **2011**, *183*, 1505–1508.
- [63] K. Takeishi, Y. Wagatsuma, H. Ariga, K. Kon, K. Shimizu, *ACS Sustain. Chem. Eng.* **2017**, *5*, 3675–3680.
- [64] H. Ham, J. Kim, S. J. Cho, J. Choi, D. J. Moon, J. W. Bae, *ACS Catal.* **2016**, *6*, 5629–5640.
- [65] H. Ham, S. W. Baek, C. H. Shin, J. W. Bae, *ACS Catal.* **2019**, *9*, 679–690.
- [66] Z. Li, J. Li, M. Dai, Y. Liu, D. Han, J. Wu, *Fuel* **2014**, *121*, 173–177.
- [67] J. W. Jung, Y. J. Lee, S. H. Um, P. J. Yoo, D. H. Lee, K. W. Jun, J. W. Bae, *Appl. Catal. B: Environ.* **2012**, *126*, 1–8.
- [68] R. J. D. Silva, A. F. Pimentel, R. S. Monteiro, C. J. A. Mota, *J. CO₂ Util.* **2016**, *15*, 83–88.
- [69] S. Baek, S. Kang, J. W. Bae, Y. Lee, D. Lee, K. Lee, *Energy Fuels* **2011**, *25*, 2438–2443.

- [70] C. Zeng, J. Sun, G. Yang, I. Ooki, K. Hayashi, Y. Yoneyama, A. Taguchi, T. Abe, N. Tsubaki, *Fuel* **2013**, *112*, 140–144.
- [71] R. Khoshbin, M. Haghghi, *Catal. Sci. Technol.* **2014**, *4*, 1779–1792.
- [72] J. Sun, G. Yang, Q. Ma, I. Ooki, A. Taguchi, T. Abe, Q. Xie, Y. Yoneyama, N. Tsubaki, *J. Mater. Chem. A* **2014**, *2*, 8637–8643.
- [73] G. Yang, N. Tsubaki, J. Shamoto, Y. Yoneyama, Y. Zhang, *J. Am. Chem. Soc.* **2010**, *132*, 8129–8136.
- [74] Y. Wang, W. Wang, Y. Chen, J. Ma, R. Li, *Chem. Eng. J.* **2014**, *250*, 248–256.
- [75] Y. Wang, W. Wang, Y. Chen, J. Ma, J. Zheng, R. Li, *Chem. Lett.* **2013**, *42*, 335–337.
- [76] Y. Q. Sun, X. H. Han, Z. K. Zhao, *Catal. Sci. Technol.* **2019**, *9*, 3763–3770.
- [77] C. Jeong, H. Ham, J. W. Bae, D. C. Kang, C. H. Shin, J. H. Baik, Y. W. Suh, *ChemCatChem* **2017**, *9*, 4484–4489.
- [78] G. Yang, D. Wang, Y. Yoneyama, Y. Tan, N. Tsubaki, *Chem. Commun.* **2012**, *48*, 1263–1265.
- [79] G. Yang, M. Thongkam, T. Vitidsant, Y. Yoneyama, Y. Tan, N. Tsubaki, *Catal. Today* **2011**, *171*, 229–235.
- [80] G. Yang, C. Xing, W. Hirohama, Y. Jin, C. Zeng, Y. Suehiro, T. Wang, Y. Yoneyama, N. Tsubaki, *Catal. Today* **2013**, *215*, 29–35.
- [81] W. Ding, M. Klumpp, S. Lee, S. Reuß, S. A. Al-Thabaiti, P. Pfeifer, W. Schwieger, R. Dittmeyer, *Chem. Ing. Tech.* **2015**, *87*, 702–712.
- [82] K. Pinkaew, G. Yang, T. Vitidsant, Y. Jin, C. Zeng, Y. Yoneyama, N. Tsubaki, *Fuel* **2013**, *111*, 727–732.
- [83] R. Phienluphon, K. Pinkaew, G. Yang, J. Li, Q. Wei, Y. Yoneyama, T. Vitidsant, N. Tsubaki, *Chem. Eng. J.* **2015**, *270*, 605–611.
- [84] C. Dai, A. Zhang, M. Liu, X. Guo, C. Song, *Adv. Funct. Mater.* **2015**, *25*, 7479–7487.
- [85] M. Behrens, *J. Catal.* **2009**, *267*, 24–29.

Entry for the Table of Contents (Please choose one layout)

FULL PAPER

Simple but efficient: This work reports a new and highly efficient capsule-structured CuO-ZnO-Al₂O₃@HZSM-5 catalyst for direct conversion of syngas to dimethyl ether by a facile physical coating method with ethanol as a binder, it shows 2.9 times higher CO conversion with 2.7 times higher TOF and 9.2 times higher dimethyl ether space-time yield of CZA@HZSM-5 catalyst with silica sol as a binder (315.5 vs 34.3 g DME kg cat⁻¹ h⁻¹).



Yongle Guo and Zhongkui Zhao*

Page No. – Page No.

Ethanol as a Binder to Fabricate a Highly-Efficient Capsule-Structured CuO-ZnO-Al₂O₃@HZSM-5 Catalyst for Direct Production of Dimethyl Ether from Syngas

Accepted Manuscript